Supporting Information

A PET-based fluorometric chemosensor for determination of mercury (II) and pH, and hydrolysis reaction-based colorimetric detection of hydrogen sulfide

Jae Jun Lee,[a] Yong Sung Kim,[a] Eunju Nam,[b] Sun Young Lee,[a] Mi Hee Lim,[b]* Cheal Kim[a]*

[a]*Department of Fine Chemistry and Department of Interdisciplinary Bio IT Materials, Seoul National University of Science and Technology, Seoul 139-743, Republic of Korea. Fax: +82-2-973-9149; Tel: +82-2-970-6693; E-mail: chealkim@seoultech.ac.kr*

[b]*Department of Chemistry, Ulsan National Institute of Science and Technology (UNIST), Ulsan 44919, Republic of Korea. Fax: +82-52-217-5409; Tel: +82-52-217-5422; E-mail: mhlim@unist.ac.kr*

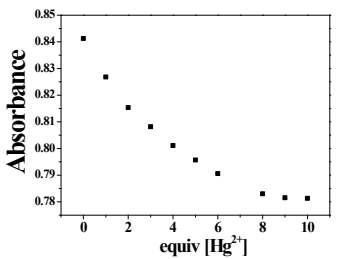

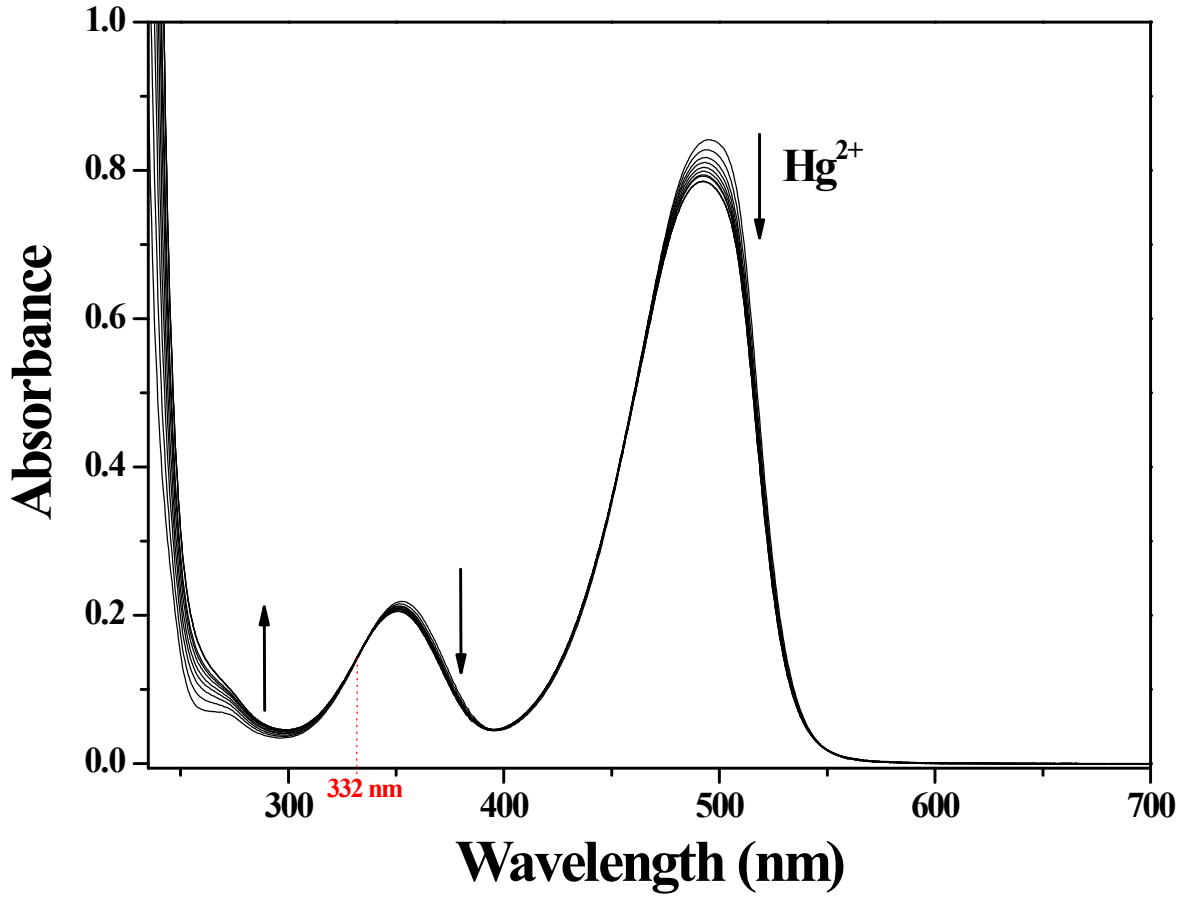

Fig. S1. Absorption spectral changes of **1** (10 μM) in the presence of increasing different concentrations of Hg^{2+} (from 0 to 10 equiv) at room temperature. Inset: Plot of the absorbance intensity at 497 nm as a function of Hg^{2+} concentration.

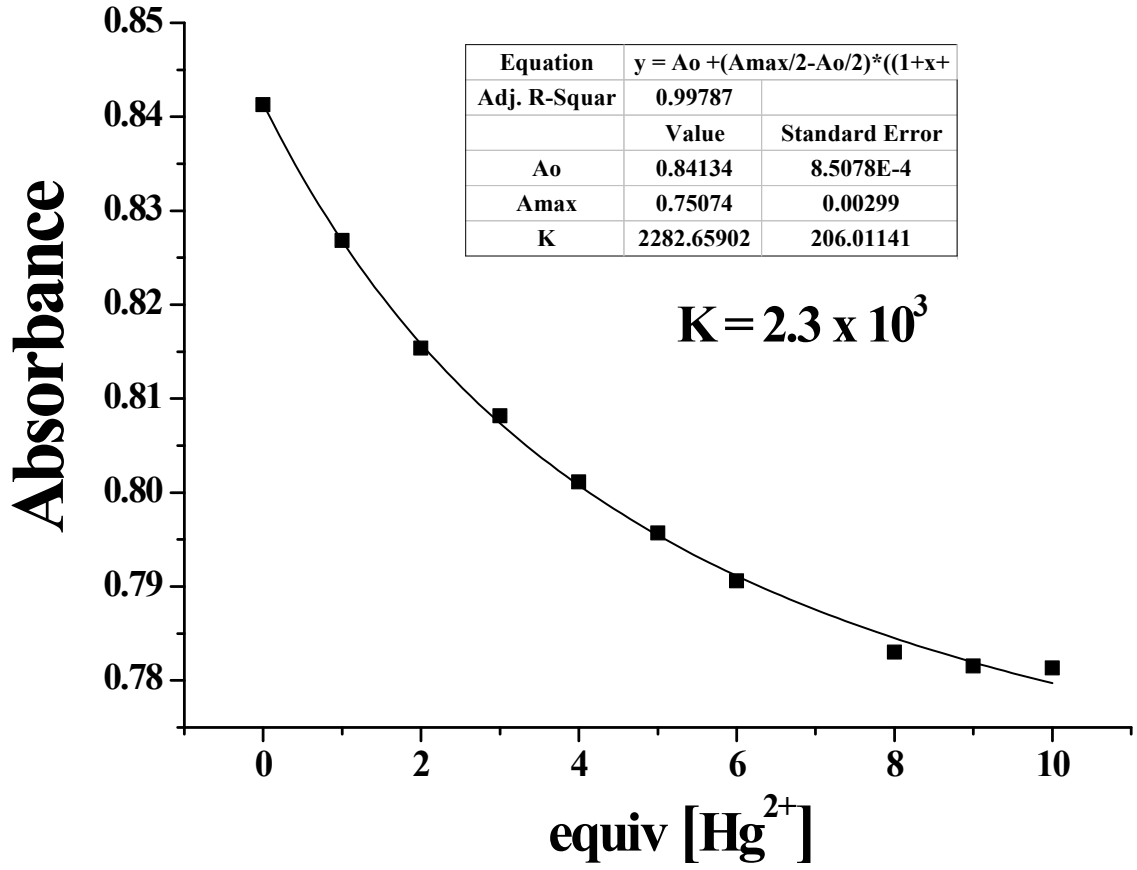

Fig. S2. Absorption intensity (at 497 nm) of **1** (10 μM) after addition of increasing different concentration of Hg^{2+} ions. The black line is the non-linear fitting curve between **1** and Hg^{2+}. Association constant (*K*) of **1** with Hg^{2+} was calculated by the non-linear least square curve fitting.

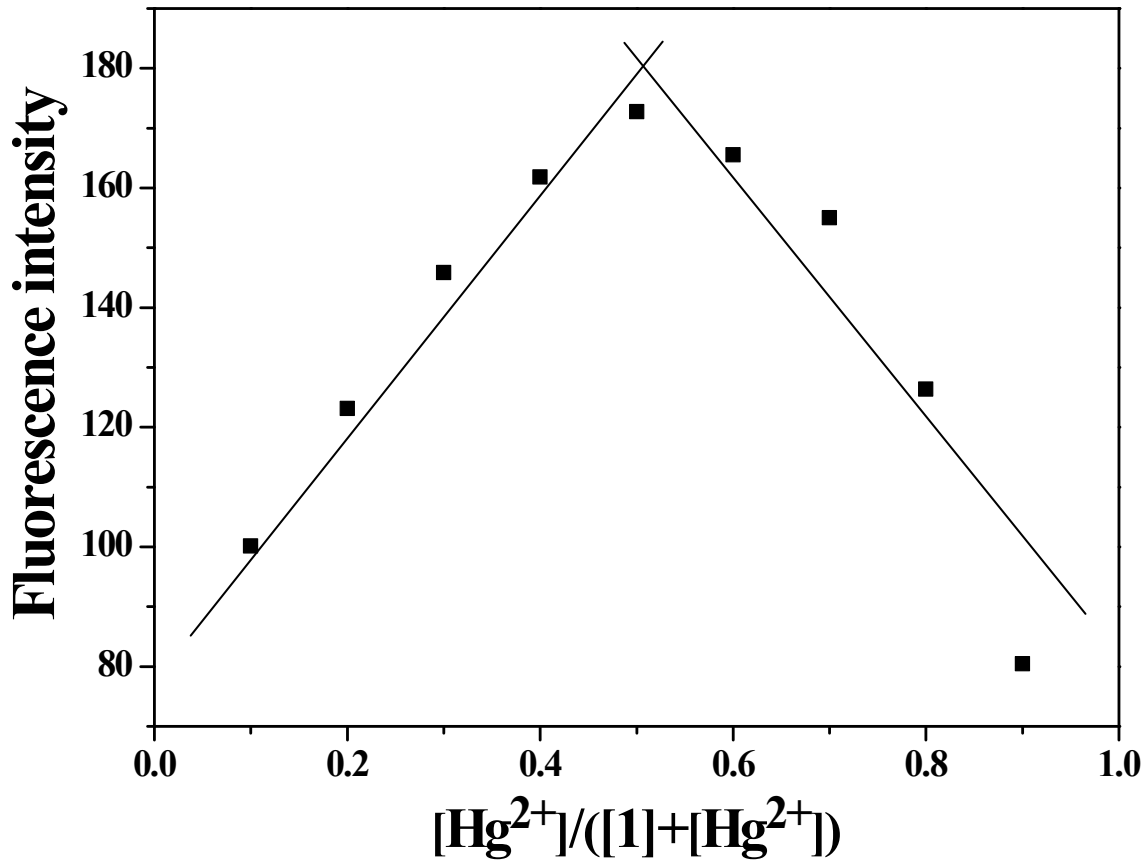

Fig. S3. Job plot for the binding of **1** with Hg^{2+}. Fluorescence intensity at 530 nm was plotted as a function of the molar ratio of $[Hg^{2+}]/([\mathbf{1}]+[Hg^{2+}])$. The total concentration of Hg^{2+} ions with receptor **1** was 1.0×10^{-5} M.

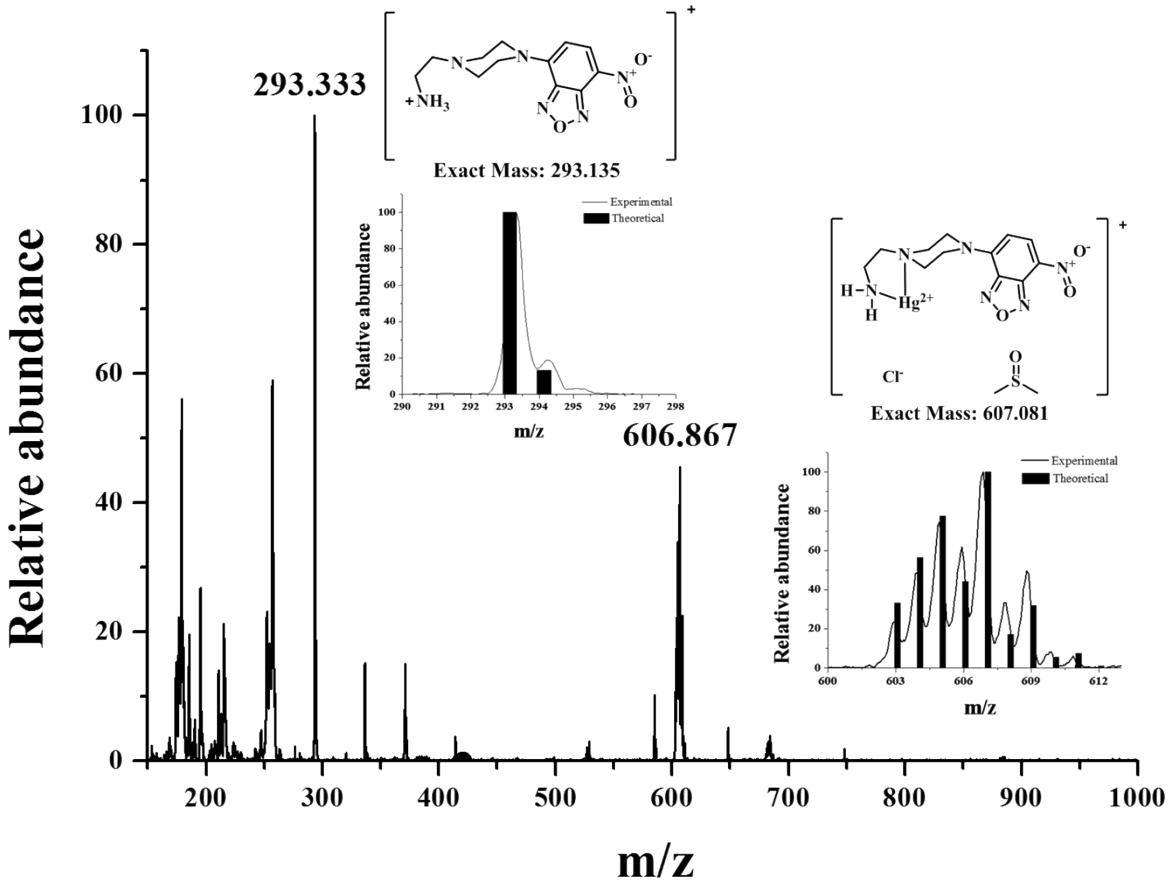

Fig. S4. Positive-ion electrospray ionization mass spectrum of **1** (10 μM) upon addition of $Hg(NO_3)_2$ (1 equiv).

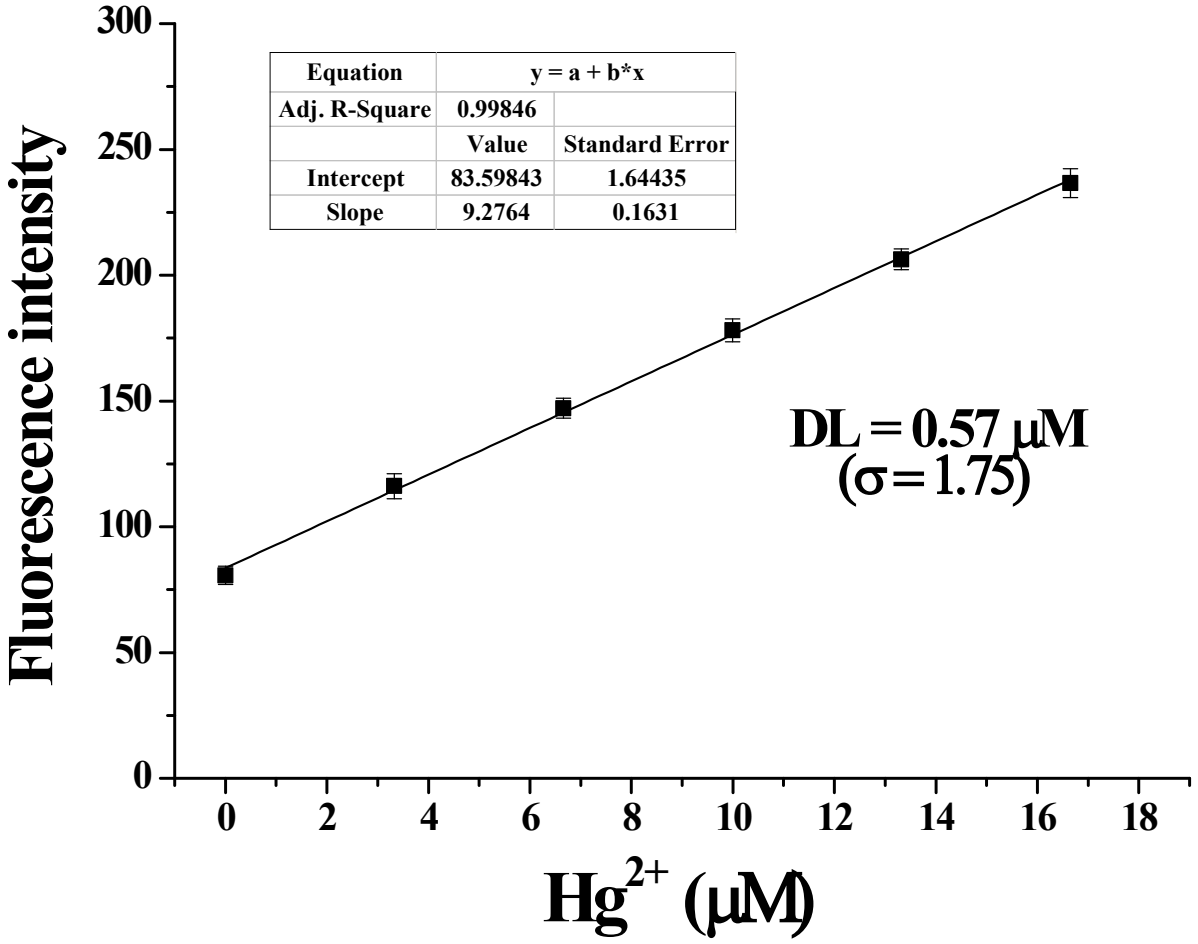

Fig. S5. Fluorescence intensity (at 542 nm) of **1** as a function of Hg^{2+} concentration in bis-tris buffer (10 mM bis-tris, pH = 7.0). [**1**] = 10 μmol/L and [Hg^{2+}] = 0-16.66 μmol/L.

(a)

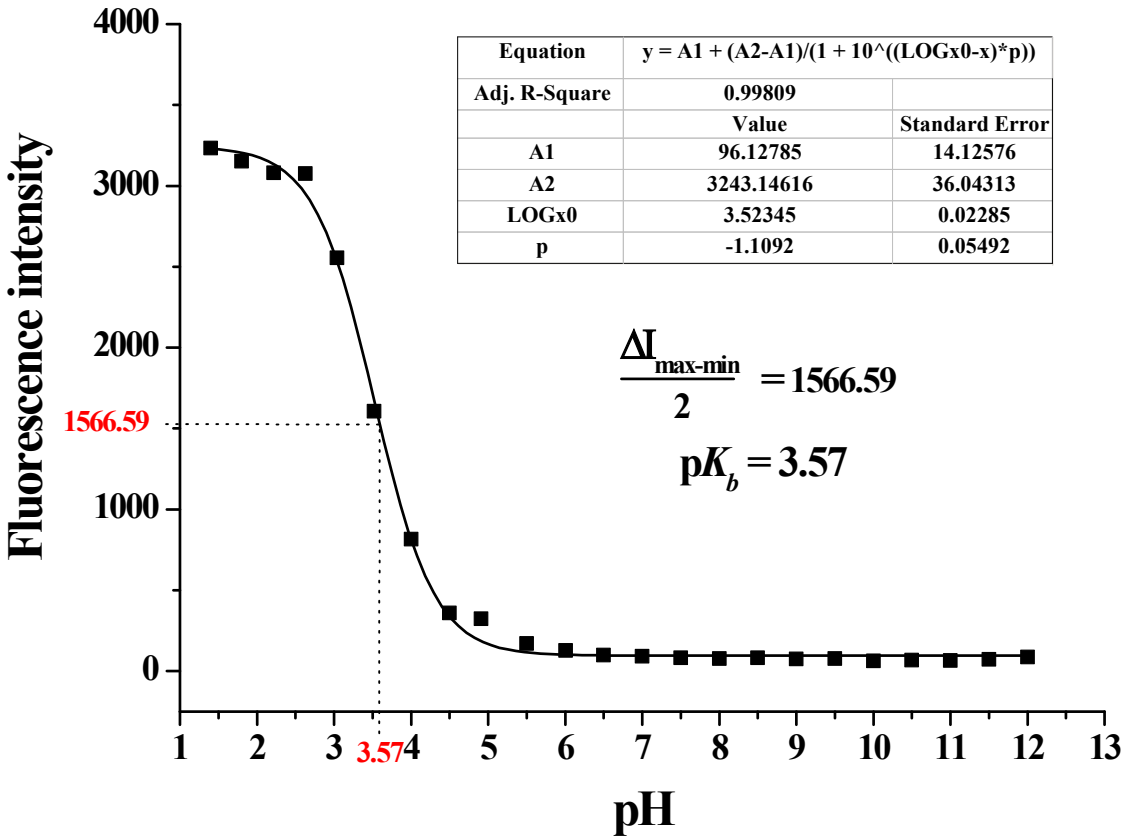

Equation	y = A1 + (A2-A1)/(1 + 10^((LOGx0-x)*p))	
Adj. R-Square	0.99809	
	Value	Standard Error
A1	96.12785	14.12576
A2	3243.14616	36.04313
LOGx0	3.52345	0.02285
p	-1.1092	0.05492

(b)

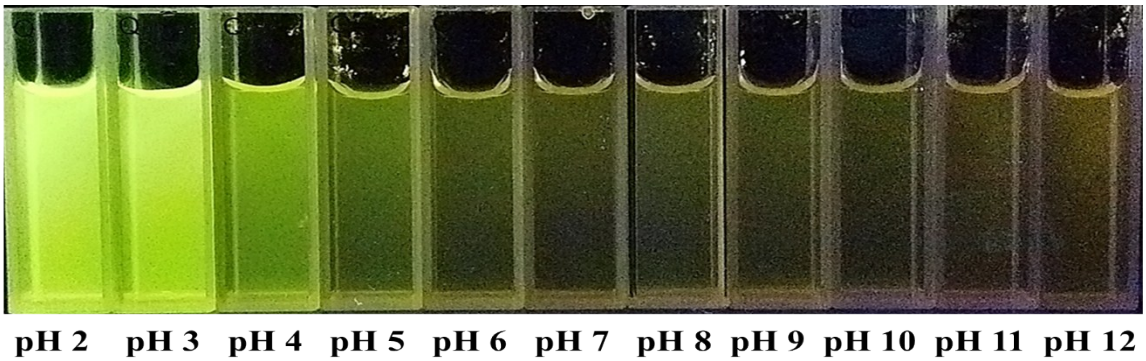

Fig. S6. (a) Fluorescence intensity (at 542 nm) of **1** (10 μM) at different pH (2-12). (b) Pictures of fluorescence color of **1** (10 μM, λ_{ex} = 365 nm) at different pH (2-12).

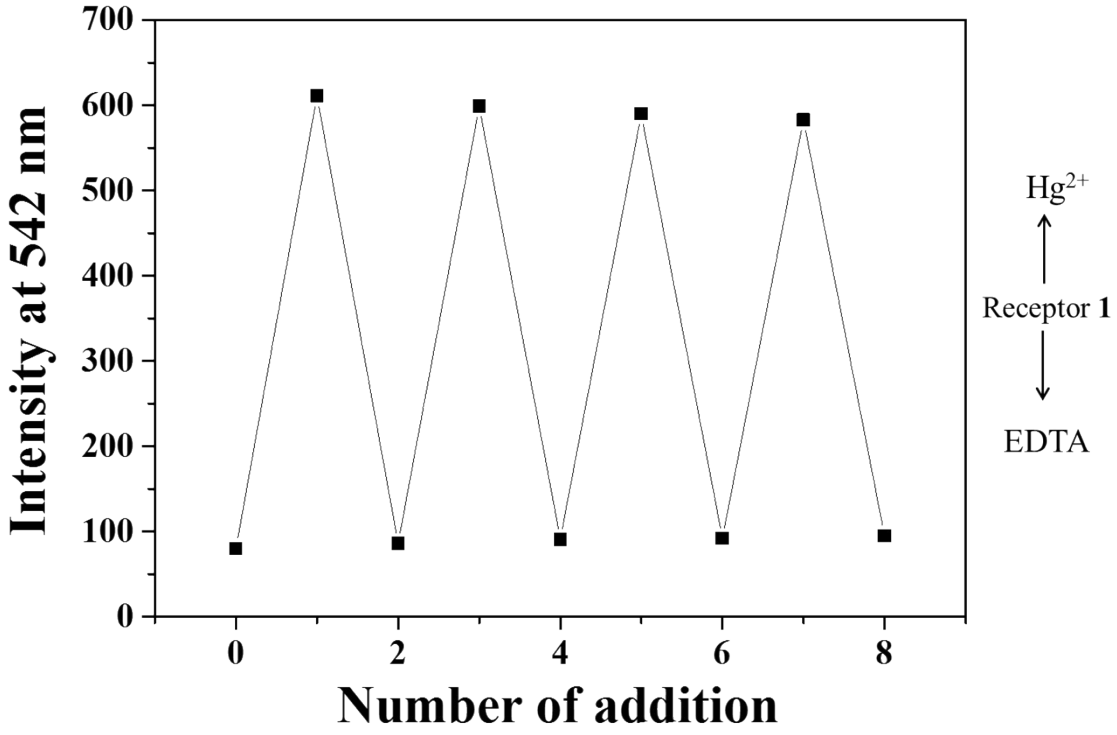

Fig. S7. Fluorescence spectral changes of **1** (10 μM) after the sequential addition of Hg^{2+} and EDTA**.**

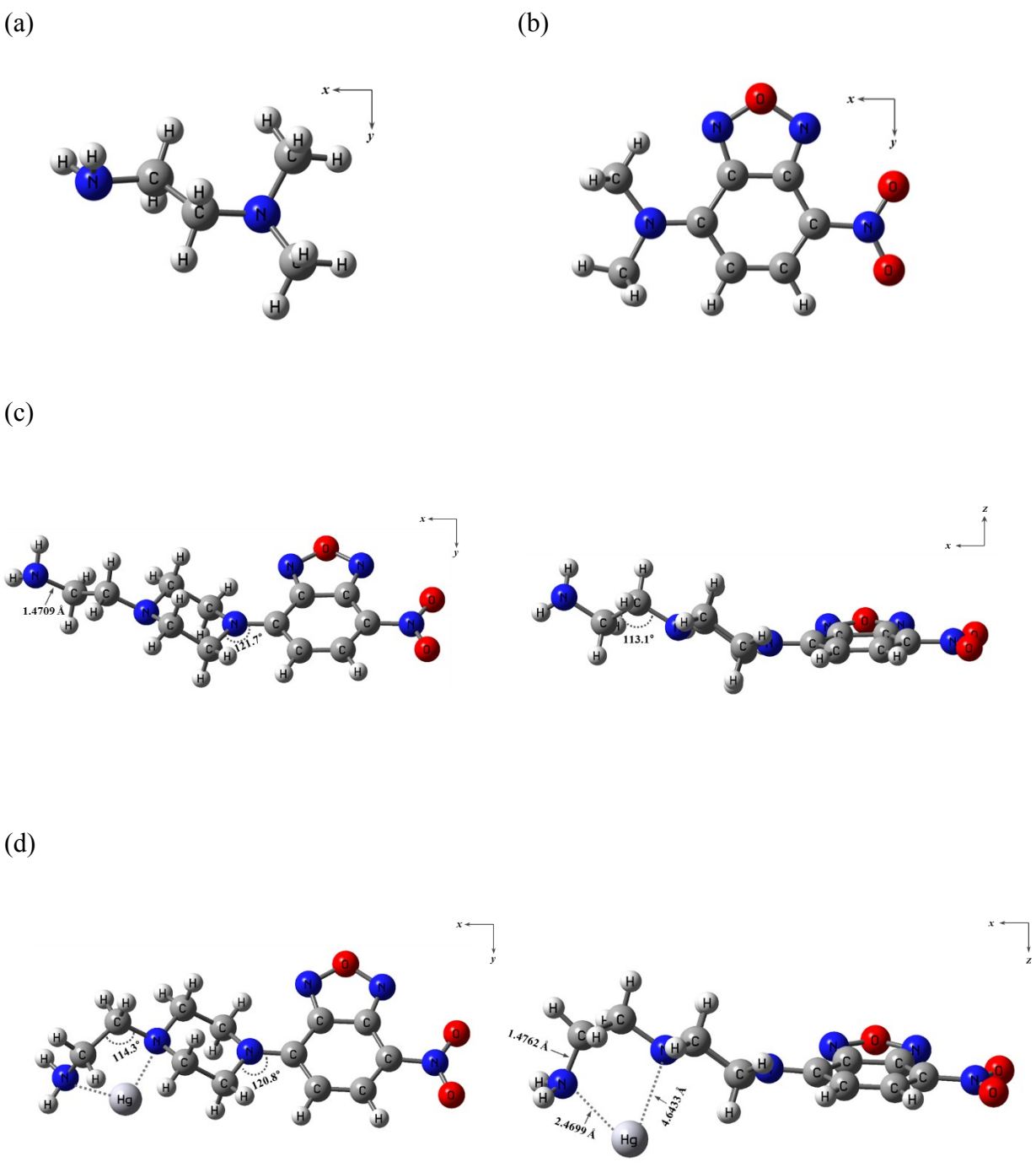

Fig. S8. Energy-minimized structures of (a) **R**, (b) **F**, (c) **1** and (d) **1**-Hg^{2+} complex from B3LYP level.

(a)

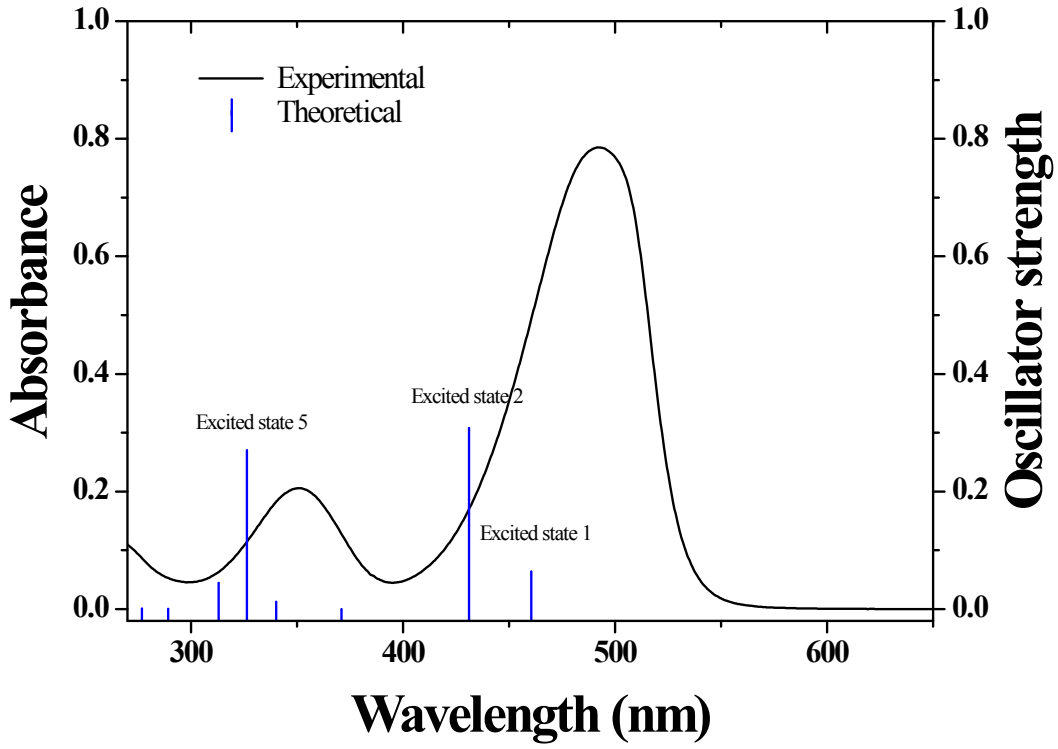

(b)

Excited State 1	Wavelength	percent	Oscillator strength
H → L	460.48 nm	55 %	0.0640
H-1 → L		44 %	
Excited State 2	**Wavelength**	**percent**	**Oscillator strength**
H-1 → L	431.04 nm	54 %	0.3079
H → L		42 %	
H → L+1		3 %	
Excited State 5	**Wavelength**	**percent**	**Oscillator strength**
H → L+1	326.43 nm	95 %	0.2703
H → L		3 %	

Fig. S9. (a) The theoretical excitation energies and the experimental UV-vis spectrum of **1**. (b) The major electronic transition energies and molecular orbital contributions for **1** (H = HOMO

and L = LUMO).

(a)

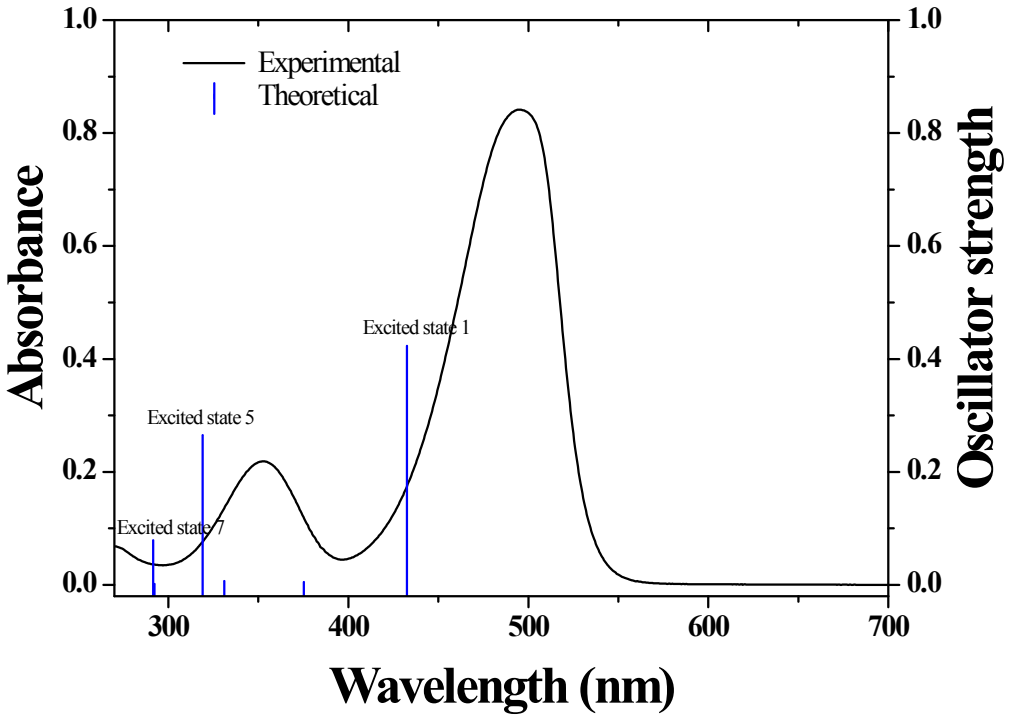

(b)

Excited State 1	Wavelength	percent	Oscillator strength
H → L	432.51 nm	96 %	0.4230
H → L+2		3 %	
Excited State 5	**Wavelength**	**percent**	**Oscillator strength**
H → L+2	318.98 nm	94 %	0.2654
H → L		3 %	
Excited State 7	**Wavelength**	**percent**	**Oscillator strength**
H-1 → L+1	291.46 nm	95 %	0.0788

Fig. S10. (a) The theoretical excitation energies and the experimental UV-vis spectrum of **1**-Hg^{2+}. (b) The major electronic transition energies and molecular orbital contributions for **1**-Hg^{2+} (H = HOMO and L = LUMO).

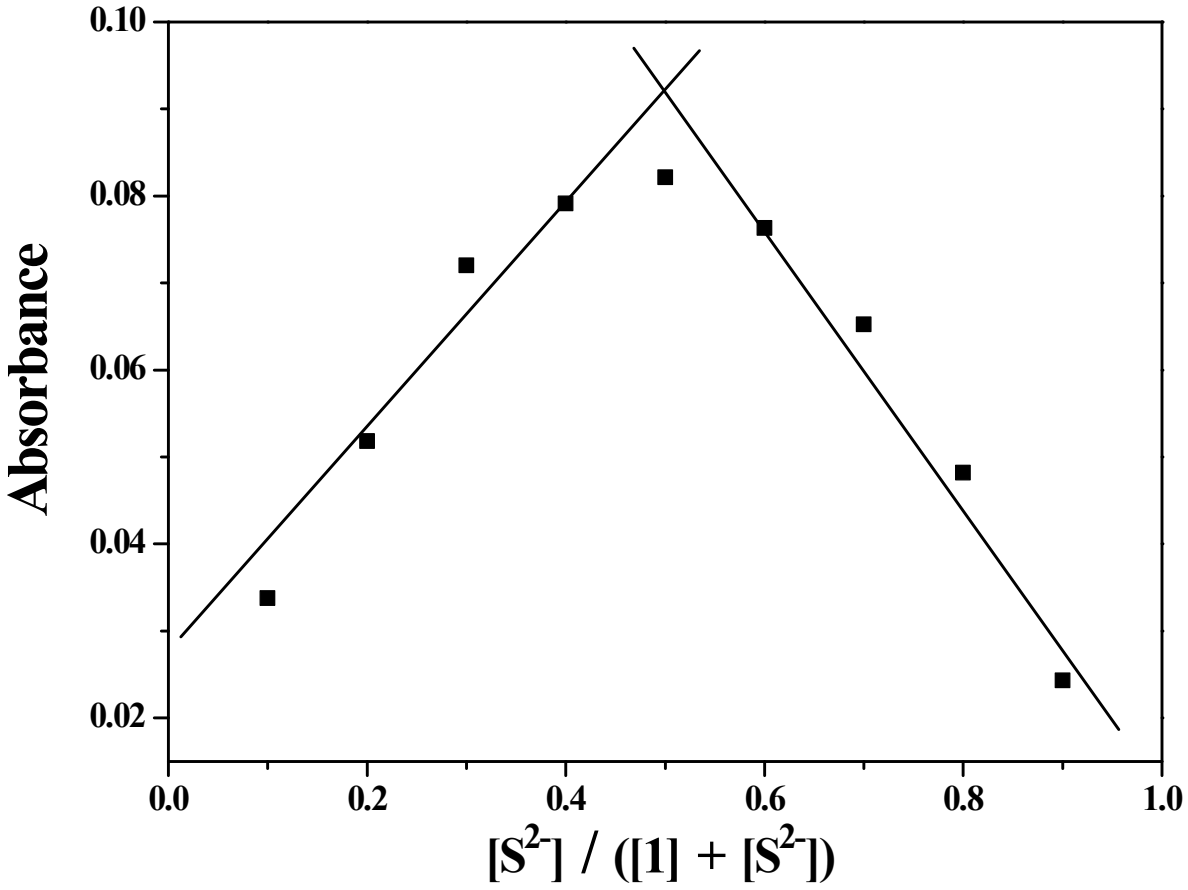

Fig. S11. Job plot for the binding of **1** with S^{2-}. Absorption intensity at 350 nm was plotted as a function of the molar ratio of $[S^{2-}]/([\mathbf{1}]+[S^{2-}])$. The total concentration of S^{2-} ions with receptor **1** was 1.0 x 10^{-5} M.

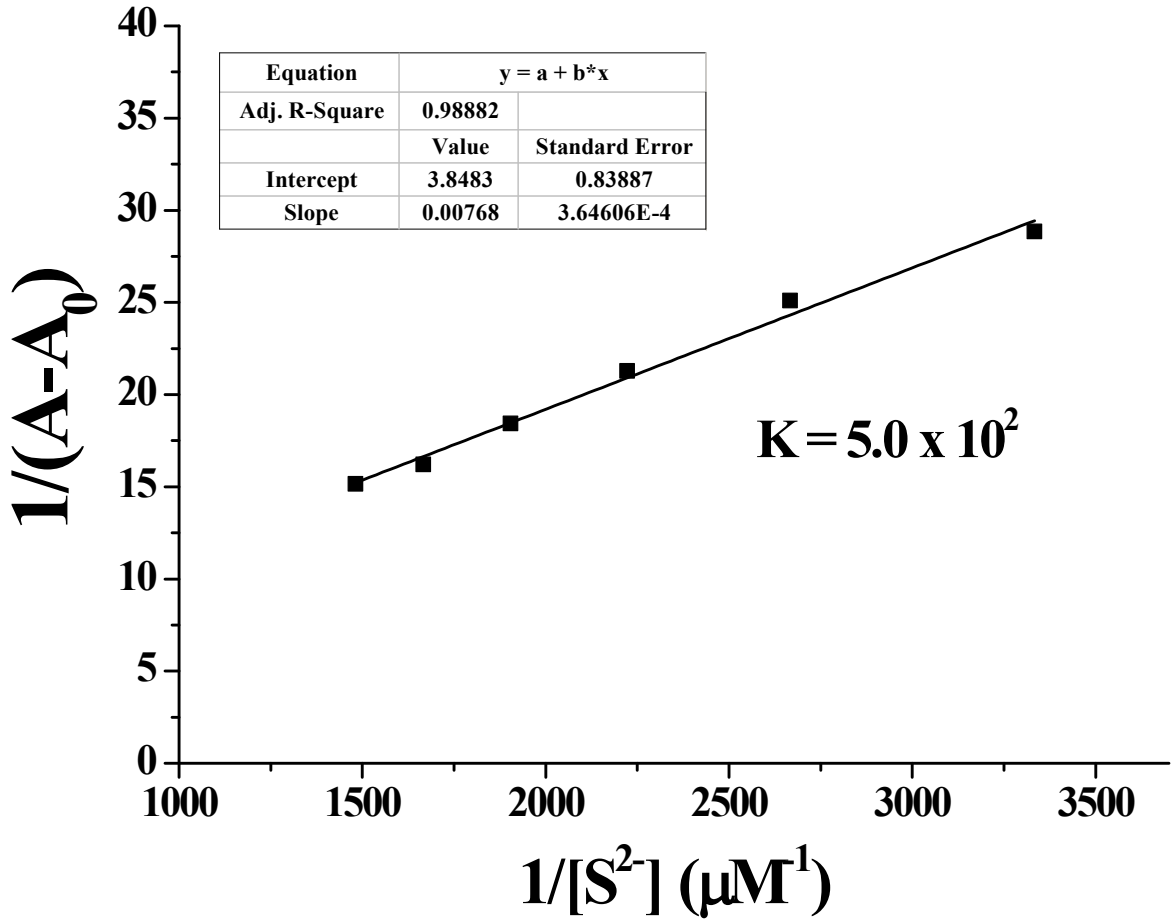

Fig. S12. Benesi-Hildebrand plot (λ_{abs} = 531 nm) of **1** (10 μM), assuming a 1:1 stoichiometry for association between **1** and S^{2-}.

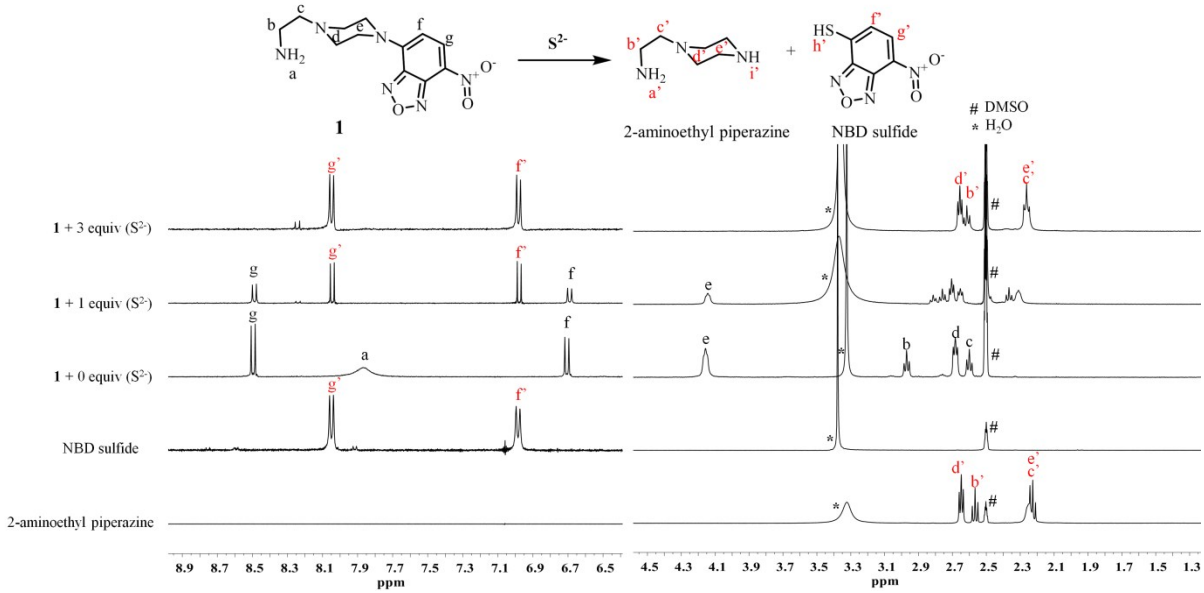

Fig. S13. ^{1}H NMR spectra of **1** upon addition of 0, 1 and 3 equiv of S^{2-}, compared with NBD-sulfide and 2-aminoethyl piperazine.

(a)

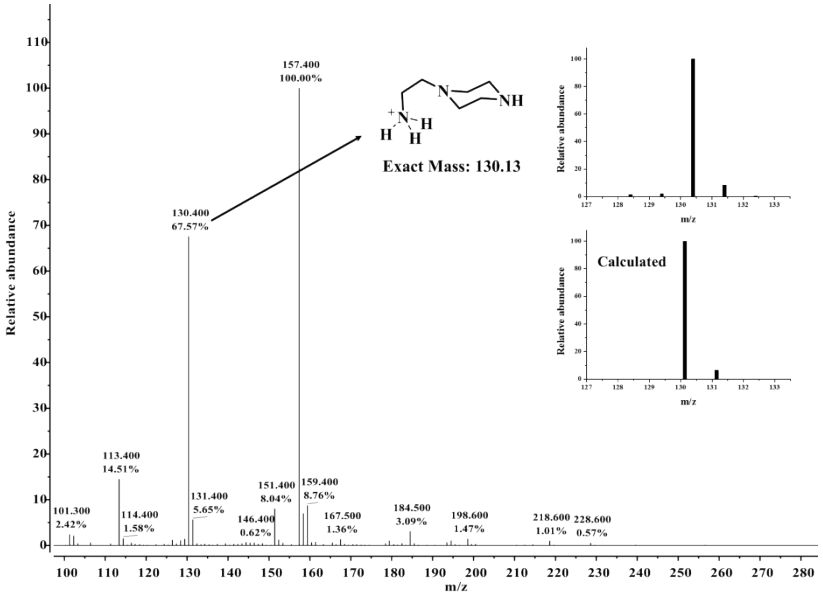
Relative abundance
m/z
157.400
100.00%
130.400
67.57%
113.400
14.51%
131.400
5.65%
151.400
8.04%
159.400
8.76%
101.300
2.42%
114.400
1.58%
146.400
0.62%
167.500
1.36%
184.500
3.09%
198.600
1.47%
218.600
1.01%
228.600
0.57%
Exact Mass: 130.13
Calculated

(b)

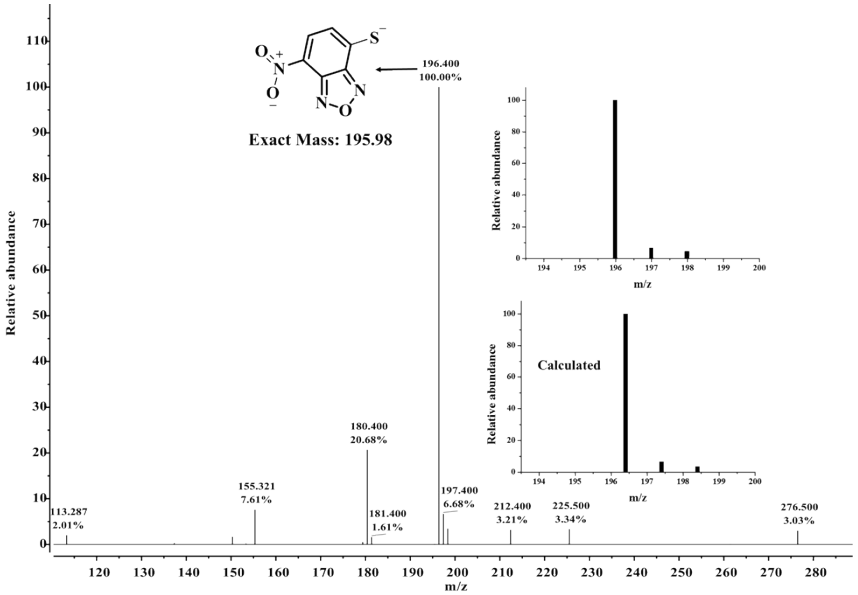
Relative abundance
m/z
196.400
100.00%
Exact Mass: 195.98
180.400
20.68%
155.321
7.61%
197.400
6.68%
113.287
2.01%
181.400
1.61%
212.400
3.21%
225.500
3.34%
276.500
3.03%
Calculated

Fig. S14. (a) Positive and (b) negative-ion electrospray ionization mass spectra of **1** (10 μM) upon addition of $Na_2S·9H_2O$ (1 equiv).

(a)

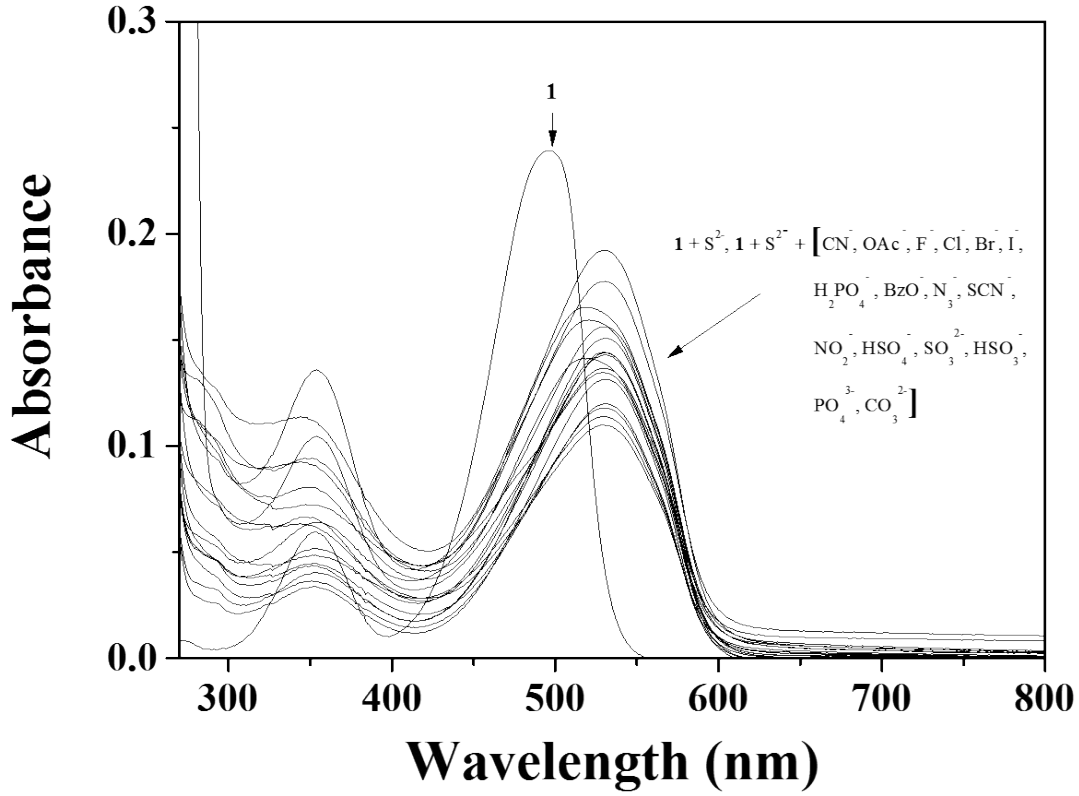

(b)

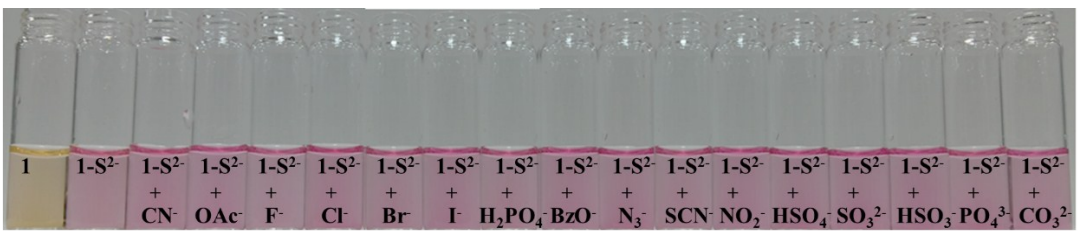

Fig. S15. (a) Absorption spectral changes of **1** (10 μM) upon addition of S^{2-} (150 equiv) in the absence and presence of 150 equiv of various anions in bis-tris buffer (10 mM, pH = 7.0). (b)

The color changes of **1** (10 μM) with S^{2-} (150 equiv) in the absence and presence of 150 equiv of various anions in bis-tris buffer (10 mM, pH = 7.0).

(a)

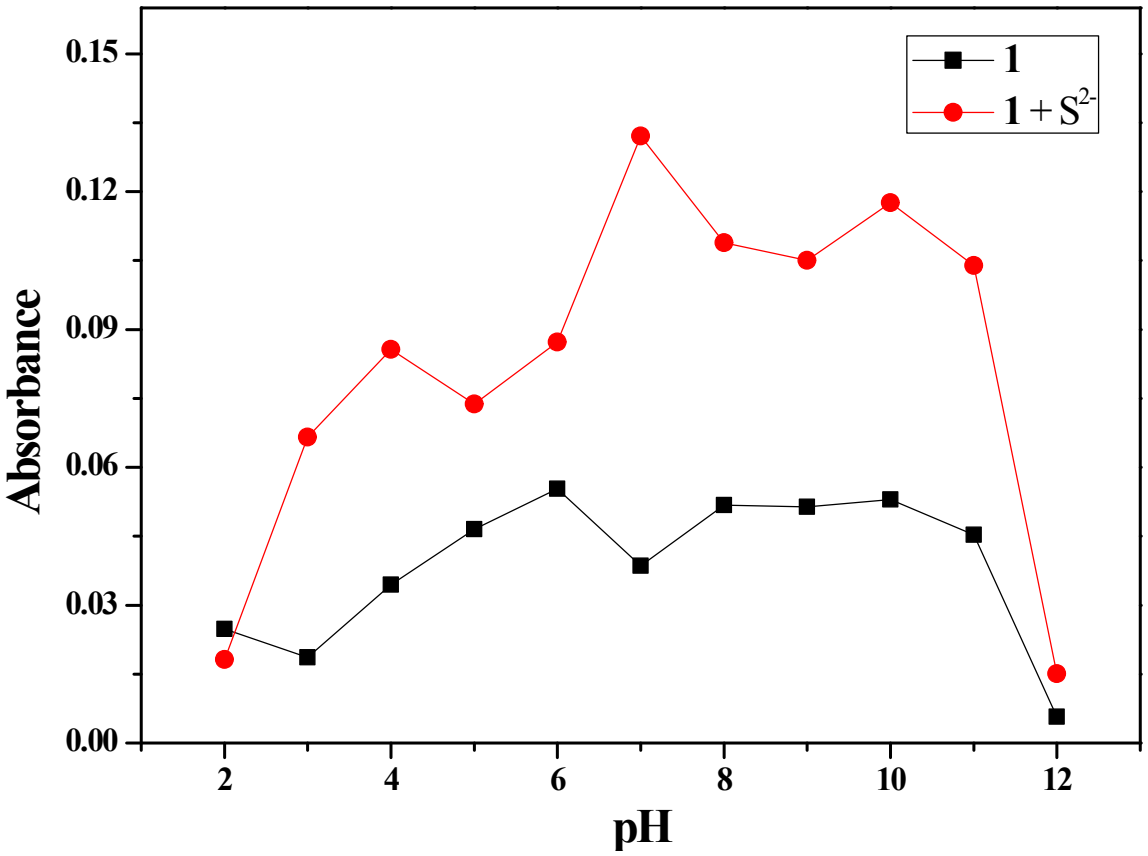

(b)

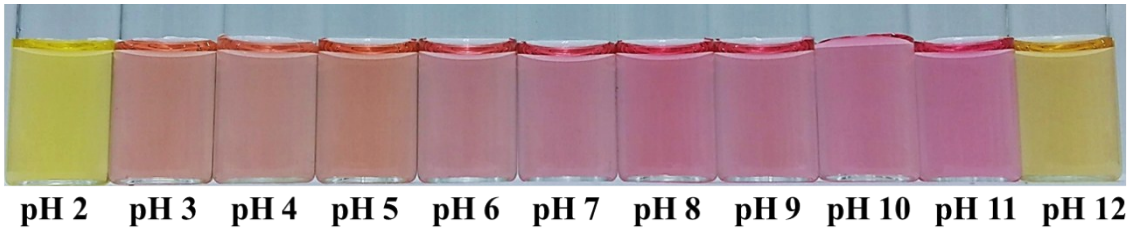

Fig. S16. (a) Absorbance (at 531 nm) of **1** and **1**-S^{2-} (**1**: 10 μM, S^{2-}: 150 equiv) at different pH (2-12). (b) The color changes of **1**-S^{2-} (**1**:10 μM, S^{2-}: 150 equiv) at different pH (2-12).

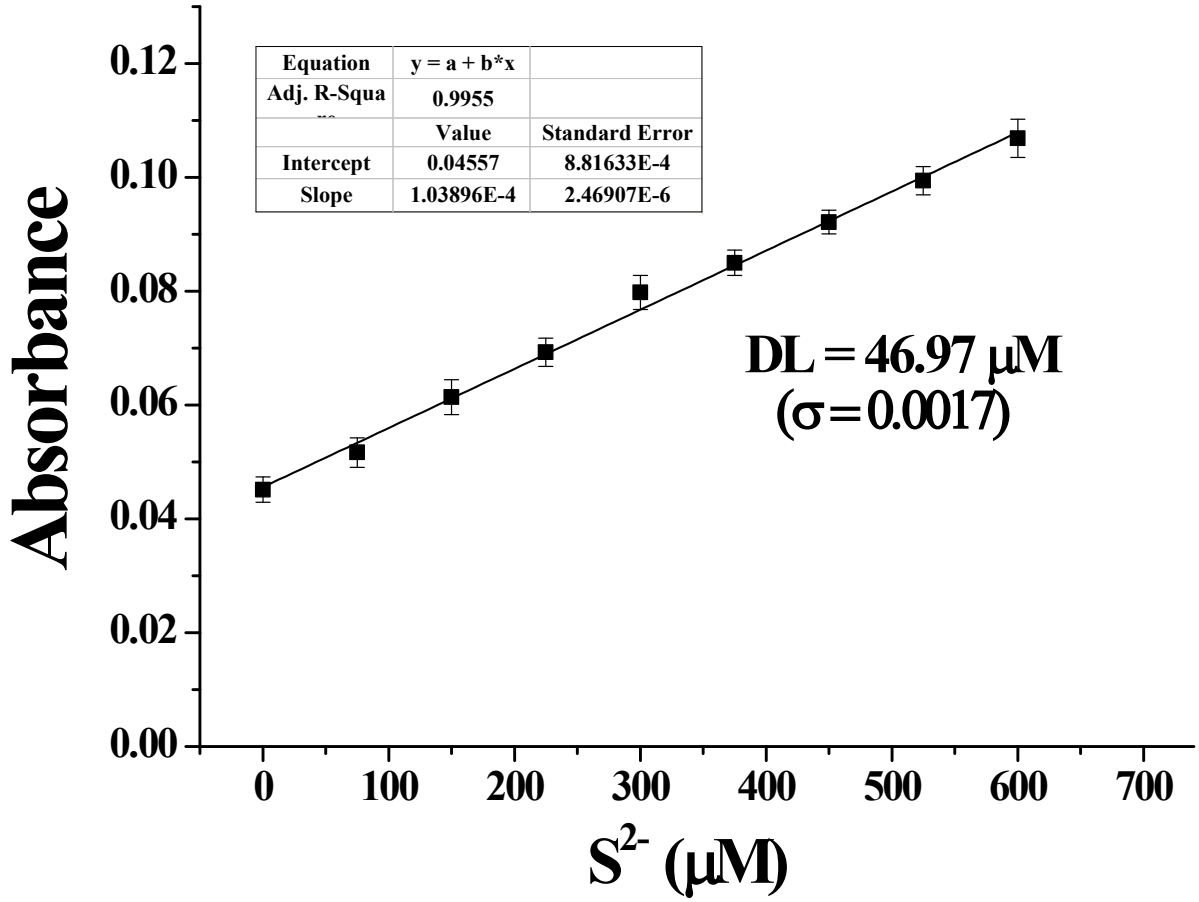

Fig. S17. Absorption intensity (at 531 nm) of **1** as a function of S^{2-} concentration in bis-tris buffer (10 mM bis-tris, pH = 7.0). [**1**] = 10 μmol/L and [S^{2-}] = 0-600 μmol/L.